International Journal of Medical, Medicine and Health Sciences
ISSN: 2517-9969
Vol:6, No:1, 2012

Shape Memory alloy Actuator System Optimization for New Hand Prostheses

Mogeeb A. Ahmed, Mona F. Taher, and Sayed M. Metwalli

***Abstract*—**Shape memory alloy (SMA) actuators have found a wide range of applications due to their unique properties such as high force, small size, lightweight and silent operation. This paper presents the development of compact (SMA) actuator and cooling system in one unit. This actuator is developed for multi-fingered hand. It consists of nickel-titanium (Nitinol) SMA wires in compact forming. The new arrangement insulates SMA wires from the human body by housing it in a heat sink and uses a thermoelectric device for rejecting heat to improve the actuator performance. The study uses optimization methods for selecting the SMA wires geometrical parameters and the material of a heat sink. The experimental work implements the actuator prototype and measures its response.

***Keywords*—**Optimization, Prosthetic hand, Shape memory alloy, Thermoelectric device, Actuator system

I. Introduction

SMAs are metallic materials having the ability to return to a previously determined shape when heated to or above their transition temperature. This occurs because the heat causes the material to pass from the weak martensite phase to the more rigid austenite phase, which is known as the "shape memory effect" [1]. One of the most common SMAs is Nitinol (NiTi). The (NiTi) thin wire contracts when a voltage is applied to their ends. The advantages of NiTi wires include their extremely small size, volume etc. [1, 2, 3]. Their main disadvantages as prosthetic actuators are: (a) the high temperatures required for transition, which result in a relatively slow recovery time until cooling occurs [4], and (b) the small strains they produce (3% - 8%) require extensive lengths of wire for large strains sufficient to flex the fingers. Several prosthetic hands actuated by SMAs have been proposed in the literature [1, 5]. These hands suggested embedding SMA wires in the palm [5, 6] or in the arm. Ref.[4] presented a direct attaching of SMA to the finger structure.

The proposed SMA actuator uses (NiTi) multiple wires in a compact arrangement, which overcomes the size limitation. The actuator will be designed to generate a force that reaches up to 15 N and a stroke that reaches up to 20mm. This force is sufficient to mimic the natural fingertip force. These SMA wires will be cooled to improve the actuator response.

M. A. Ahmed is a PhD candidate with Cairo University, Egypt; (e-mail: mogeebahmed2@ masrawy.com).
M. F. Taher, is with the Department of Biomedical Engineering Systems, Cairo University, Egypt (e-mail: taher.mona@gmail.com).
S. M. Metwalli is with the Mechanical Design and Production Department, Cairo University, Egypt, (e-mail:metwallis2@asme.org).

The cooling system consists of a heat sink and a thermoelectric (TE) device [7].

The SMA actuator and cooling system unit will be placed in a separate modular component for the proposed prosthetic hand. The design and analysis of that multi-fingered anthropometric prosthetic hand were explained in a separate paper by the authors [8]. Herein, the design parameters of the actuation system and heat sink material are determined using optimization. The study implements the actuator prototype and the experimental work aims at verifying the mathematical modeling and the effect of different cooling systems.

II. SMA Compact Actuator And Cooling System Design

SMA Nitinol (NiTi) wires (Dynalloy, Inc.) are selected as the actuator for their pre-described advantages. The challenge was to propose a design that uses these advantages and overcomes the drawbacks, which include the small stroke and the slow cooling. The stroke (4% strain) dictated a long length of wire to achieve the tendon excursion needed for sufficient finger flexion. This was overcome by designing the initial compact arrangement as shown in Fig.1. The SMA wires are routed around Teflon rollers to reduce friction and the spring is required to provide the SMA bias force that well be determined by optimization. This in turn will dictate the spring characteristics.

A cooling or recovery time of the SMA increases with the increase of the cross-sectional area of the wire. However, the actuation force also increases with the cross-sectional area thus posing the challenge of selecting the optimum cross-section, which will allow sufficient force within the constraints of reasonable recovery times. The geometrical dimensions of the SMA wires will be determined by the optimization described hereafter. To improve the cooling rate, the cooling system is designed to include a heat sink and a TE device. This particular cooling system is composed of a thermoelectric (TE) device and two aluminium heat sinks as shown in Fig.1. The TE device used is PE127-14-15 S [7]. The first heat sink is used for the housing of the SMA wires and is cooled by the TE device. The second heat sink is for rejecting the heat of the TE device.

In previous studies [9-11], the optimization of heat sink design parameters are based on minimization of the mass and maximization of both rejected and stored heat. These studies considered the relevant design parameters including geometric constraints, heat dissipation and material properties of the heat

sink [9-11]. The SMA actuator in this study uses a heat sink with standard dimensions. So, the optimization role herein will be to determine the optimum material of the heat sink in addition to other system parameters.

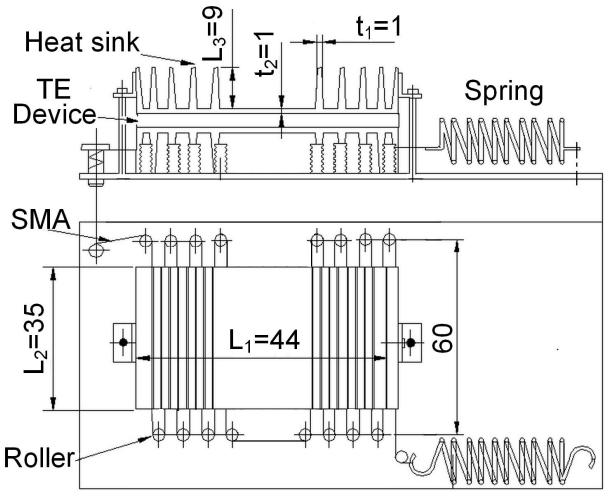

Fig. 1 Compact actuator and cooling system module

III. Actuator Design Formulation

SMA is actuated by resistive heating of the SMA wires with step current, *I* in Ampere. The temperature *T* along the wire is uniform and is obtained from the following relation.

$$\rho_{SMA} V c \frac{dT}{dt} = I^2 R_{SMA} - h A_s (T - T_o) \quad (1)$$

Where R_{SMA} is the electrical resistance of SMA wire, ρ_{SMA} is the density of the SMA, *V* is the volume of SMA wire, *h* is the convection heat transfer coefficient, A_s is the surface area of the SMA wire, *c* is the specific heat and T_o is the ambient temperature. The differential equation (Eq.1), considers that the heat transmission occurs by air convection and neglects the radiation effect [14].

The cooling system is analyzed using a lumped concept to get the equivalent thermal resistance circuit [15]. This concept assumes the temperature is varied with time and uniform within the heat sink dimensions. Fig.2 shows the equivalent thermal circuit of the planned cooling system. The components R_1, R_2, and R_3 are the thermal resistances of the heat sink. R_c is the thermal contact resistance between SMA wire and heat sink. $R_{3\text{-amb}}$ is the thermal resistance between the heat sink and the air. R_h is the thermal resistance between the SMA wire and the air. The distribution of thermal resistances on the cooling system is shown in Fig.3. C_{SMA}, and C_{hs} are the equivalent thermal capacitances of the SMA wire and the heat sink respectively. They are related to the specific heat and volume.

R_c is defined by.

$$R_c = \frac{2}{h_c \pi n D_{SMA} L_{SMA}} \quad (2)$$

Where h_c is the thermal conductance of the contact between SMA and heat sink, *n* is the number of wires, D_{SMA} is the SMA wire diameter and L_{SMA} is the SMA wire length.

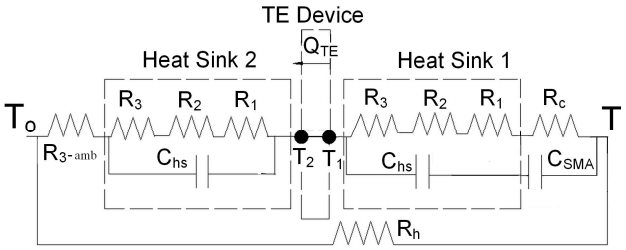

Fig. 2 Equivalent thermal resistance circuit for SMA with TE device and heat sink

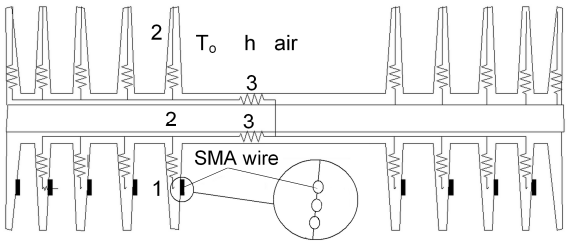

Fig. 3 Distribution of thermal resistances on the cooling system

R_h is defined by

$$R_h = \frac{2}{h \pi n D_{SMA} L_{SMA}} \quad (3)$$

R_1, R_2, and R_3 are the thermal resistances at point 1, point 2 and point 3 respectively as shown in Fig.3. These resistances are defined by.

$$R_1 = \frac{2t_1}{k_{Al}\, n \pi D_{SMA} L_{SMA}}, \quad (4)$$

$$R_2 = \frac{L_3}{N\, k_{Al}\, L_2\, t_1}, \quad (5)$$

$$R_3 = \frac{t_2}{k_{Al}\, L_1 L_2} \quad (6)$$

Where t_1, t_2, L_1, L_2 and L_3 are the geometrical dimensions of the heat sink as shown in Fig.1, *N* is the number of fins and k_{Al} is the Aluminum conductivity.

$R_{3\text{-amb}}$ is the thermal resistance between the heat sink, and ambient air. The following relation defines it.

$$R_{3-amb} = \frac{1}{h(L_2 L_2 + N L_2 t_2)} \quad (7)$$

The cooling system will be analyzed by the lumped concept. The cooling system has both conductive and convective heat transmission. This system is analogous an integrator circuit.

The SMA cooling with heat sink system is expressed by the following ODE.

$$C_{eq} \frac{dT}{dt} = I^2 R_{SMA} - \frac{(T - T_o)}{R_{eq1}} \quad (8)$$

Where

$$R_{eq1} = \frac{(R_c + R_1 + R_2 + R_3 + R_{3-amb}) R_h}{R_c + R_1 + R_2 + R_3 + R_{3-amb} + R_h} \quad (9)$$

and

$$C_{eq} = \frac{C_{hs} C_{SMA}}{C_{hs} + C_{SMA}} \quad (10)$$

The solution of Eq.8 for the heating stage is given by.

$$T_h = T_o + \frac{w}{R_{eq1}}[1-\exp(-Dt)] \quad (11)$$

Where $D = \frac{1}{C_{eq}R_{eq1}}$.

And for the cooling stage the solution is given by

$$T = T_o + (T_h - T_o)[\exp(-Dt)] \quad (12)$$

The initial SMA wire temperature is $T(0) = T_o$ and the steady–state value of the SMA wire temperature T_{ss} for a step current when $\frac{dT}{dt}=0$ is $T_{ss}=\frac{w}{R_{eq}}$.

The cooling with TE device and heat sink is analyzed by using superposition. The hot side temperature of TE device T_2 is determined by.

$$C_{hs}\frac{dT_2}{dt} = Q_{TE} - \frac{(T_2 - T_o)}{R_{eq2}} \quad (13\text{-a})$$

Where Q_{TE} is the rejected heat of TE device and

$$R_{eq2} = \frac{(R_1 + R_2 + R_3 + R_{3-amb})R_h}{R_1 + R_2 + R_3 + R_{3-amb} + R_h} \quad (13\text{-b})$$

From the specifications of the TE device, there is a temperature difference ΔT_{TEM} between the hot and cold sides of the TE device. The cold side temperature T_1 is

$$T_1 = T_2 - \Delta T_{TEM} \quad (14)$$

Therefore, the SMA temperature T is defined by

$$C_{eq}\frac{dT}{dt} = -\frac{(T - T_1)}{R_{eq1}} \quad (15)$$

Phase kinetics depends on Ikuta's Model [10,12] to obtain the martensite fraction R_m. It describes the behaviour of the major hystersis curve as an exponential curve. The martensite fraction $R_{m(h,c)}$ for heating and cooling is defined by

$$R_{m(h,c)} = \frac{1}{1+e^{K_{m(h,c)}(T-\gamma_{(h,c)})}} \quad (16)$$

Where K_{mh} and K_{mc} are related to the slope of the hysteresis curve through heating and cooling, γ_h and γ_c are related to the transformation temperatures and additionally include the effect of stress on the hysteresis curve. They are expressed at cooling and heating respectively by

$$\gamma_h = \frac{1}{2}(a_s + a_f) - T_o + C_m(\sigma - \sigma_o) \quad (17)$$

$$\gamma_c = \frac{1}{2}(m_s + m_f) - T_o + C_m(\sigma - \sigma_o) \quad (18)$$

Where m_S, m_f, a_s, a_f are transformation temperatures of the SMA. C_m and σ_o are the effect of stress on transformation temperatures, and the initial stress respectively [6]. The pretension stress σ_1 of SMA at cooling phase is given by

$$\sigma_1 = \frac{F_1}{A_c} \quad (19)$$

Where A_c is the cross-sectional area of SMA wire and F_1 is the bias force. The resultant effective elasticity E_{eff} is given by

$$E_{eff} = R_m(E_m) + (1-R_m)E_a \quad (20)$$

Where E_a is the austenite elasticity and E_m is the martensite elasticity of SMA.

Therefore the strain at cooling phase is given by.

$$\varepsilon_1 = \frac{\sigma_1}{E_m} \quad (21)$$

The stress σ_2 at the heating phase is given by

$$\sigma_2 = \frac{F_1 + df}{A_c} \quad (22)$$

Where df is the actuation force.

The strain at point heating phase is

$$\varepsilon_2 = \frac{\sigma_2}{E_{eff}} \quad (23)$$

The model assumes that the SMA is linear in the martensite (cooling) and austenite (heating) phase.

The mechanical work density of the SMA W_{SMA} is expressed by.

$$W_{SMA} = \frac{1}{2}(\varepsilon_2 - \varepsilon_1).(\sigma_1 - \sigma_2) \quad (24)$$

For the heat sink material selection, the design of the heat sink considers the maximization of rejected (dissipated) heat Q_{rej}, the stored heat Q_{stored} and also the minimization of the heat sink mass m.

The mass of the heat sink is defined by

$$m = \rho.V_{hs} \quad (25)$$

Where ρ is the density of heat sink material and V_{hs} is the volume of the heat sink.

The stored heat capacity Q_{stored} of the cooling system is defined by

$$Q_{stored}=(T-T_o).C_{eq} \quad (26)$$

The rejected heat Q_{rej} from SMA is defined by

$$Q_{rej} = \frac{T - T_o}{R_{eq1}} \quad (27)$$

Table I shows the mass, rejected heat and stored heat of the same heat sink dimensions with different materials.

TABLE I
DIFFERENT HEAT SINK MATERIALS ANALYSIS

Material	Heat sink mass (g)	Rejected heat (W/m^2)	Stored heat (W)
Aluminum	12	0.0224	5.8593
Copper	35	0.0425	19.1772
Silver	55	0.046	21.7034

IV. System Optimization

In this section, the design variables, objective function, and the constraints of the optimization are defined. The design variables are SMA wire cross-sectional area, number of wires, the bias force, and the material of heat sink properties, conductivity, specific heat and density. In this study, the geometrical parameters of the heat sink are kept constant. The objective function f is defined as:

$$f = \frac{\text{Mass of the heat sink}}{[\text{Rejected heat} + \text{Stored heat capacity}].[\text{Work density of the SMA}]} \quad (28)$$

The constraints include the following: the yield stresses and the elastic modules of the SMA at the martensite and the austenite phases. The maximum strain of the SMA at the martensite phase is less than 4% [3]. The constraints are

related to the property values of heat sink materials.The constraints related to the property values of the heat sink metals are such as density ρ, specific heat C and thermal conductivity K. There is another constraint on the diameter of SMA wire.

The heat sink material properties are constrained within the following ranges.

$$10000 > \rho > 2700 \ \frac{Kg}{m^3}, \tag{29}$$

$$400 > K > 200 \ \frac{W}{m\ K^{o}}, \tag{30}$$

$$880 > C > 200 \ \frac{J}{kg\ .K^{o}} \tag{31}$$

The SMA wire diameter is constrained within the range

$$0.5 > D_{SMA} > 0.05mm \tag{32}$$

The optimization problem is defined as a classical non-linear optimization problem with constraints. The solution is obtained by the Sequential Quadratic Programming method (SQP) that is implemented by the function *fmincon* of MATLAB Optimization Toolbox [13]. The function *fmincon* finds the minimum of a constrained nonlinear multivariable objective function f [16] and determines the optimum constrained design variables.

V. Experimental Work

The SMA actuator and cooling system unit as shown in Fig.1 is implemented with the specifications and optimization results that is shown in Table I. The prototype is implemented for actuating one finger as shown in Fig. 4. In the experimental work the used SMA wire length is 400mm. This is the available commercial length by Dynalloy [3]. The experimental work measures the response of the actuator with different cooling methods and its load capacity. The study uses linear variable differential transformer (LVDT), Data acquisition card Velleman K8055 and Battery (6 V-1.2 A) as shown in the layout of the experimental setup defined schematically in Fig. 5.

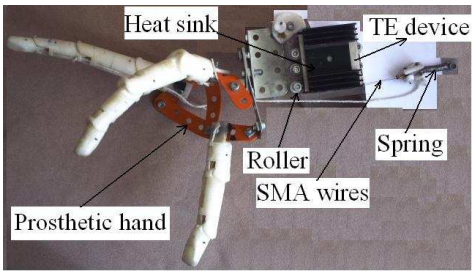

Fig. 4 Prototype for actuating one hand prostheses finger

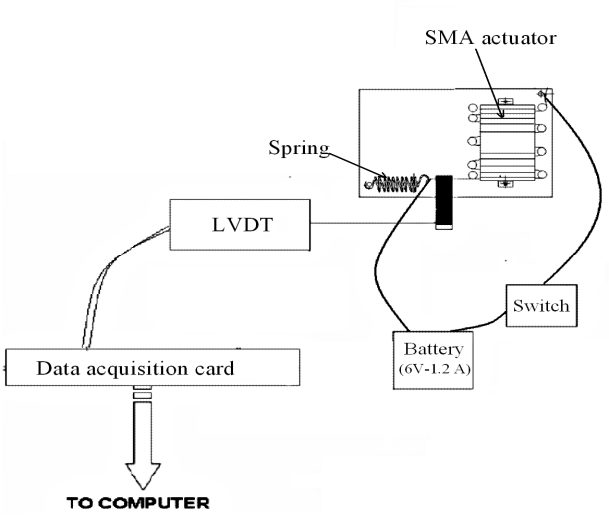

Fig. 5 Layout of the experimental setup

VI. Results

Table II shows optimum design variables of SMA actuator. To evaluate the effect of forced cooling on the relaxation rate a simulation was performed using Eq.1, which describes the cooling rate in an ambient air. Simulations were repeated for cooling with a heat sink alone using Eq.8, and for cooling with the heat sink and a TE device using Eq.13. The simulations are carried out for the contraction and relaxation of the 400 mm of SMA wire with a diameter of 0.15 mm at an excitation current of 1.2 A for a duration of 1s. Fig. 6 and Fig. 7 show the simulation results of SMA actuator with various cooling methods. Fig. 6 is the same as Fig. 7 but with shifted start to clarify the outcome. The smooth lines are for the simulation results and the jiggled or wrinkled lines are for the experimental ones. Experimentally, the implemented actuator has a 10 mm stroke and a lift of 1.3 Kg.

TABLE.II
Optimum SMA Actuator Parameters

Bias force (N)	Wire area (mm^2)	Heat sink material	No. of wires	Load capacity (N)	Temp (C^o)	Stroke (mm)
3.2	0.09	Aluminum	6	15	100	20

VII. Discussion

The current design proposes a compact solution for the required long length of SMA wires. In previous studies, this length is fitted in the forearm, or routed in the palm [5] or finger [6]. Forced cooling in this study using heat sinks and the TE device is more suitable for biomedical applications than forced air, oil or water. TE device cooling has previously been used in prosthetic hand [17] but not in a compact form and other works [5, 6] do not use cooling.

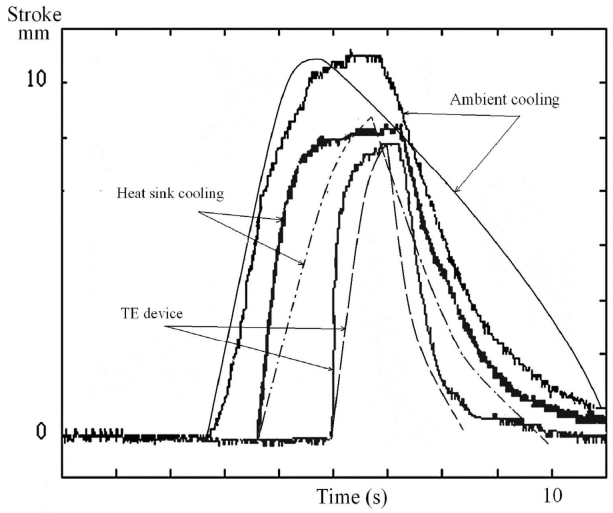

Fig. 6a Comparison between the analytical and experimental results with shifted start to clarify the outcome

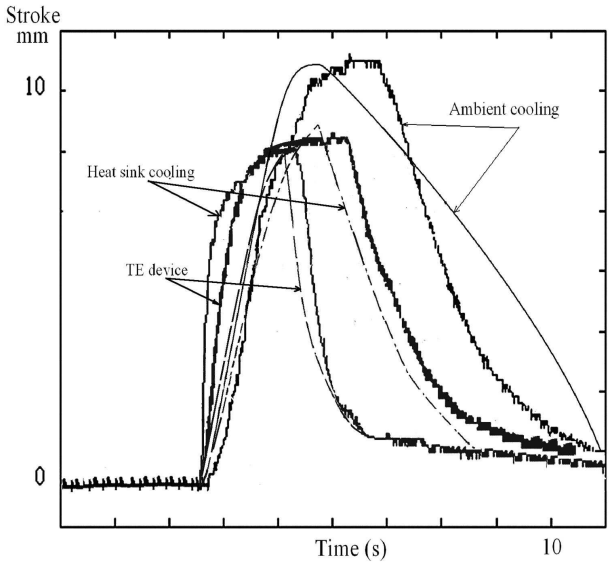

Fig. 6b Different cooling methods effect with results at the same start to indicate the effectiveness of cooling

In the developed optimum cooling system design, the ratio between cross sectional area and surface area of SMA wires should be large. For this reason a large number of thinner SMA wires are used. This optimum cooling system improves the relaxation rate of the actuators than without cooling as shown in Fig. 6.

Fig. 5 shows the difference between the analytical and experimental results. The SMA simulation used the phenomenological model that assumes the wire resistance is constant and the elastic modulus is linear in both phases. Furthermore, the cooling system used the lumped analysis (the temperature is varied with time only) to simplify the modelling and assumed the rejected heat of the TE device is linear with the consumed current. The modelling neglected the friction effect between the wires and the rollers, that causes backlash as shown in Fig. 5, and reduces the load capacity of the implemented actuator than the designed. The case of ambient cooling is conforming more to the experiments in the literature [18 and 19]. Forced cooling is clearly more effective.

VIII. Conclusion

The developed actuator overcomes the usual SMA wires for hand prostheses that requires long wire or large space to generate the sufficient stoke and adequate response. The optimum actuation module is a compact arrangement of SMA wires, which is cooled using a heat sink and thermoelectric (TE) device. The forced cooling improves the actuator performance by rejecting the SMA heat. The optimum design minimizes the heat sink weight and defines the optimum parameters of the actuation system and also provides the optimum material selection of the heat sink. The prototype actuator is implemented for actuating one finger. The experimental work verifies the analytical results of the prototype with different cooling methods. The optimum actuating system with forced cooling is clearly advantageous.

References

[1] V.O. Del Cura, "A Study of the Different Types of Actuators and Mechanisms for upper limb prostheses," *Artificial Organs*, 2003, pp: 507–516.

[2] C.S. Loh; H. Yokoi; T. Arai, "New Shape Memory Alloy Actuator: Design And Application In The Prosthetic Hand," *Proceedings Of The 2005 IEEE Engineering In Medicine And Biology 27th Annual Conference Shanghai*, China, 2005.

[3] Dynalloy, Inc: http://www.dynalloy.com. Accessed on 2011.

[4] K.J. De Laurentis; C. Mavroidis, "Mechanical Design Of A Shape Memory Alloy Actuated Prosthetic Hand," *Technology And Health Care*, 2002, pp: 91–106.

[5] K.T. O'Toole; M.M Mcgrath, "Mechanical Design And Theoretical Analysis Of A Four Fingered Prosthetic Hand Incorporating Embedded SMA Bundle Actuators," *Proceedings Of World Academy Of Science Engineering And Technology*, 2007.

[6] V. Bundhoo; E. Haslam; B. Birch; E. A. Park, "Shape Memory Alloy-Based Tendon-Driven Actuation System For Biomimetic Artificial Fingers, Part I: Design And Evaluation," *Robotica* , April 2008, pp:131–146.

[7] European thermodynamics: http://www.europeanthermodynamics.com. Accessed on 2011.

[8] M.A. Ahmed; M.F. Taher; S.M. Metwalli, "New optimum humanoid hand design for prosthetic applications," *International Journal of Artificial Organs*, Initial Acceptance October 2011.

[9] S. Z. Shuja, "Optimization Of A Finned Heat Sink Array Based On Thermoeconomic Analysis," *Int. J. Energy Research*, 2007, pp: 455–471.

[10] M.D. Rakib, "Optimization of Heat Sinks with Flow Bypass Using Entropy Generation Minimization", Msc. University of Waterloo, 2006.

[11] W.A. Khan; M. M. Yovanovich; J.R. Culham, "Optimization of Microchannel Heat Sinks Using Entropy Generation Minimization Method", IEEE Transactions on Components and Packaging Technologies, 2009, Vol. 32 pp: 243 – 251

[12] K. Ikuta; M. Tsukamoto; S. Hirose, "Mathematical model and experimental verification of shape memory alloy for designing micro actuator," in Proceedings of IEEE MEMS, Nara, Japan, 1991, pp. 103–108.

[13] T. Coleman; M.A.Yin Zhang, "Optimization Toolbox for Use with MATLAB R2007b," The MathWorks: Natick, MA, USA, 2007.

[14] A. Pai, "A phenomenological model of shape memory alloys including time-varying stress," *Master of Science*, Waterloo Press, 2007.

[15] A. Trivedi, "Thermo-Mechanical Solutions in Electronic Packaging: Component to System Level," *Master of Science*, Texas Press, 2008.

[16] F. De Bona; M.G.H. Munteanu, "Optimized flexural hinges for compliant micromechanism," *Analog integrated circuits and signal processing*, 2005, pp: 163–174.
[17] K. Cho; H.H. Asada, "Architecture Design Of A Multiaxis Cellular Actuator Array Using Segmented Binary Control Of Shape Memory Alloy," *IEEE Transactions On Robotics*, August 2006.
[18] MJ. Mosley and C Mavroidis, "Experimental Nonlinear Dynamics of a Shape Memory Alloy Wire Bundle Actuator," Journal of Dynamic Systems, Measurement, and Control, 2001: pp 103-112.
[19] M Mertmann and G Vergani, "Design and application of shape memory actuators. Eur. Phys. J. Special Topics," 2008 (158): pp 221–230.